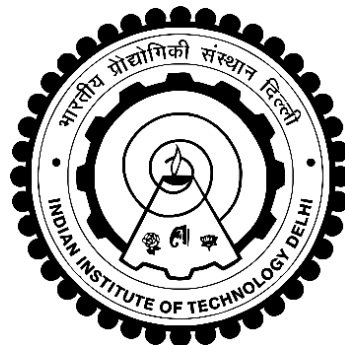


SEISMIC FRAGILITY OF LONG-SPAN SPECIAL TRUSS MOMENT FRAMES WITH MULTI-PANEL DUCTILE SEGMENTS

RAJESH KUMAR



**DEPARTMENT OF CIVIL ENGINEERING
INDIAN INSTITUTE OF TECHNOLOGY DELHI**

SEPTEMBER, 2021

©Indian Institute of Technology Delhi (IITD), New Delhi, 2021

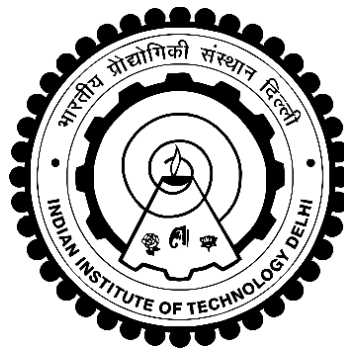
SEISMIC FRAGILITY OF LONG-SPAN SPECIAL TRUSS MOMENT FRAMES WITH MULTI-PANEL DUCTILE SEGMENTS

by

RAJESH KUMAR

Department of Civil Engineering

*Submitted
in fulfilment of the requirements of the degree of Doctor of Philosophy
to the*



INDIAN INSTITUTE OF TECHNOLOGY DELHI

SEPTEMBER, 2021

CERTIFICATE

This is to certify that the thesis entitled, “*Seismic Fragility of Long-Span Special Truss Moment Frames with Multi-Panel Ductile Segments*” being submitted by *Rajesh Kumar* to the Indian Institute of Technology Delhi, for the award of degree of *Doctor of Philosophy* is a bonafide record of research work carried out by him under our supervision and guidance. The thesis, in our opinion has reached the requisite standard, fulfilling the requirements for the award of degree of *Doctor of Philosophy*.

The research report and results presented in this thesis have not been submitted, in part or full, to any University or Institute for the award of any degree or diploma.

Prof. Dipti Ranjan Sahoo
Professor
Department of Civil Engineering
Indian Institute of Technology Delhi
Hauz Khas, New Delhi-110016 (INDIA)

Prof. Ashok Gupta
Professor
Department of Civil Engineering
Indian Institute of Technology Delhi
Hauz Khas, New Delhi-110016 (INDIA)

ACKNOWLEDGEMENTS

I would like to express my deepest gratitude to my supervisors, Prof. Dipti Ranjan Sahoo and Prof. Ashok Gupta who have been very consistent in guiding me over the past 7 years. This research work would not have been possible without their guidance, continuous support, and positive criticism, throughout the entire period of research during PhD. Their mentoring has been exceptional. Because of the valuable guidance and support of my mentors, it helped me to grow as an independent researcher. Especially, Prof. Dipti Ranjan Sahoo has helped me a lot during my research through constant motivation and imparting high quality research work in a disciplined manner. It needs to be mentioned here that, Prof. Dipti Ranjan Sahoo taught me the efficient and effective way of doing research, be it conducting experiments or writing journal papers properly.

I am also thankful to my research committee members Prof. Vasant Matsagar, Prof. K. S. Rao and Prof. S. Pradyumna, for acting as my committee members even at hardship.

My sincere thanks to my seniors Dr. Ashwin Kumar, Dr. Romanbabu M. Oinam, Dr. Abhishek Verma and Dr. Ahmad Fayeeg Ghowsi for being a source of inspiration. I would like to thank my research group friends (Dr. Mohammad Adil Dar, Ruban Sugumar, Pratik Patra, Sourabh Sharma, Suraj Sahu and Gautham Anbumani) who have been very supportive and encouraging, particularly during my experimentation. They always extended their helping hand, especially during my difficult times. I am also grateful to the staff of Heavy Structures Laboratory who have worked very hard in the fabrication of my test specimens. They have been very patient in learning the fabrication of built-up members which requires immense patience.

I really enjoyed the time with the research groups especially Dr. Romanbabu M. Oinam, Dr. Abhishek Verma, Dr. Mohammad Adil Dar and Dr. Ahmad Fayege Ghowsi spent during tea breaks as there were a lot of discussion excited towards my research. I am lucky to have such a wonderful research group.

It would not be possible to complete my thesis without the support of my family. My brother, Rakesh Kumar deserves a special thanks for providing endless support during COVID-19 lockdown period. My sister, Swati Suman deserves also a special thank for providing support during writing the journal papers. I would like to express special thanks to Mrs. Manju Kumari and her daughter, Trisha Rani for providing mental and emotional support during my thesis work along with Mr. Ramanuj Kumar.

I express thanks to my dear friends (Er. Sujeet Kumar, Er. Satish Kumar, Er. Rishikesh Kumar and Er. Sanjeev Kumar etc.), who have encouraged for the pursuance towards my research.

At last, I am extremely grateful to god almighty, for blessing me with such great people, who have imparted positivity in my life.

Rajesh Kumar

ABSTRACT

Steel truss moment frames (STMFs) are used as the lateral force-resisting systems in buildings located in high seismic regions. These systems are lightweight and offer excellent lateral resistance and hysteretic energy dissipation when subjected to seismic actions. Despite of various advantages of such systems, some of the associated issues/limitations warrant for further investigation for their wider application in practice. The primary issues are the limitation on aspect ratios of Vierendeel panels, the behavior of long-span and multi-panel STMFs, the seismic collapse performance assessment of STMFs, and the behavior of STMFs with composite floor slabs. The present study aims at exploring these issues through detailed numerical and experimental investigations for achieve the enhanced seismic performance of STMFs.

Numerical models of STMFs are developed in non-linear analysis software PERFORM-3D to simulate their elastic and post-elastic behavior. The modelling parameters are validated by comparing the predicted hysteretic response with the past test results. The validated numerical models are adopted to carry out the collapse performance assessment and to determine the seismic performance factors of STMFs in accordance with FEMA P695 methodology. The numerical models of wide range of archetypes of different heights and varying aspect ratios of Vierendeel panels are developed. In addition to the nonlinear static analyses, incremental dynamic analyses are carried out for forty-four earthquake ground motions to develop the seismic fragility curves. The seismic performance was assessed through yield mechanism, drift response and rotational demand at the end of the special segments of STMF archetypes at the Design basis earthquake (DBE) and Maximum considered earthquake (MCE) ground motions. The analyses results showed that

the aspect ratio of Vierendeel panel of ductile segment could be increased to 2.5 and the height of STMFs could be increased to 65 m. while ensuring the acceptable seismic performance.

The experimental investigations were conducted on two geometrically identical STMFs with and without composite floor slabs. Panel aspect ratios of special segments of test specimens exceeded the current limitations of building codes in order to assess the cyclic performance of long-span STMFs. The main emphasis of the study on first test specimen was the yielding of the chords within the ductile segments, behavior of the elements outside the ductile segment, behavior of the columns, buckling in the flanges at the location of plastic hinges and behavior of the ductile segment. The test frame exhibited stable hysteresis response during the experiment i.e. 6% story drift. The detailing at the end of the special segment ensured the plastic hinge at the desired locations. In the second experiment, the frame with slab was also laterally loaded cyclically till 6% drift. The main emphasis of the study on frame with slab was the yielding of the chords within the ductile segments, behavior of the elements outside the ductile segment, behavior of the columns, buckling in the flanges at the location of plastic hinges, behavior of the ductile segment and crack propagation of slab. The test frame with slab also showed stable hysteresis response till 6% story drift under cyclic load. The detailing in the panel zone of the column was improved with stiffener detailing delayed the shear yielding effectively. The lateral buckling of the special segment was also delayed due to the presence of the slab. Conclusions drawn from the findings of numerical and experimental investigations are reported in this thesis.

सार

स्टील ट्रेस मोमेंट फ्रेम (एसटीएमएफ) का उपयोग उच्च भूकंपीय क्षेत्रों में स्थित इमारतों में पार्श्व बल-प्रतिरोध प्रणालियों के रूप में किया जाता है। भूकंपीय क्रियाओं के अधीन होने पर ये सिस्टम हल्के होते हैं और उत्कृष्ट पार्श्व प्रतिरोध और हिस्टेरिटिक ऊर्जा अपव्यय प्रदान करते हैं। ऐसी प्रणालियों के विभिन्न लाभों के बावजूद, कुछ संबंधित मुद्दे/सीमाएं व्यवहार में उनके व्यापक अनुप्रयोग के लिए आगे की जांच के लिए वारंट करती हैं। प्राथमिक मुद्दे वीरेंडील पैनलों के पहलू अनुपात, लंबी अवधि और बहु-पैनल एसटीएमएफ के व्यवहार, एसटीएमएफ के भूकंपीय पतन प्रदर्शन मूल्यांकन, और समग्र मंजिल स्लैब के साथ एसटीएमएफ के व्यवहार पर सीमाएं हैं। वर्तमान अध्ययन का उद्देश्य एसटीएमएफ के बढ़े हुए भूकंपीय प्रदर्शन को प्राप्त करने के लिए विस्तृत संख्यात्मक और प्रयोगात्मक जांच के माध्यम से इन मुद्दों की खोज करना है।

एसटीएमएफ के संख्यात्मक मॉडल गैर-रैखिक विश्लेषण सॉफ्टवेयर PERFORM-3D में विकसित किए गए हैं ताकि उनके लोचदार और पोस्ट-लोचदार व्यवहार का अनुकरण किया जा सके। पिछले परीक्षण परिणामों के साथ अनुमानित हिस्टेरिटिक प्रतिक्रिया की तुलना करके मॉडलिंग मापदंडों को मान्य किया गया है। फेमा पी695 कार्यप्रणाली के अनुसार पतन प्रदर्शन मूल्यांकन करने और एसटीएमएफ के भूकंपीय प्रदर्शन कारकों को निर्धारित करने के लिए मान्य संख्यात्मक मॉडल अपनाए जाते हैं। विभिन्न ऊंचाइयों के आर्कटाइप्स की विस्तृत श्रृंखला के संख्यात्मक मॉडल और वीरेंडील पैनल के अलग-अलग पहलू अनुपात विकसित किए गए हैं। गैर-रेखीय स्थैतिक विश्लेषणों के अलावा, भूकंपीय नाजुकता घटता विकसित करने के लिए चौवालीस भूकंप जमीनी गतियों के लिए वृद्धिशील गतिशील विश्लेषण किए जाते हैं। डिजाइन के आधार पर भूकंप (डीबीई) और अधिकतम माना भूकंप (एमसीई) जमीनी गतियों पर एसटीएमएफ आर्कटाइप्स के विशेष खंडों के अंत में उपज

तंत्र, बहाव प्रतिक्रिया और घूर्णी मांग के माध्यम से भूकंपीय प्रदर्शन का आकलन किया गया था। विश्लेषण के परिणामों से पता चला है कि डक्टाइल सेगमेंट के वीरेंडील पैनेल का पहलू अनुपात 2.5 तक बढ़ाया जा सकता है और एसटीएमएफ की ऊंचाई 65 मीटर तक बढ़ाई जा सकती है। स्वीकार्य भूकंपीय प्रदर्शन सुनिश्चित करते हुए।

प्रायोगिक जांच दो ज्यामितीय रूप से समान एसटीएमएफ पर मिश्रित फर्श स्लैब के साथ और बिना आयोजित की गई थी। लंबी अवधि के एसटीएमएफ के चक्रीय प्रदर्शन का आकलन करने के लिए परीक्षण नमूनों के विशेष खंडों के पैनेल पहलू अनुपात बिल्डिंग कोड की वर्तमान सीमाओं को पार कर गए हैं। पहले परीक्षण नमूने पर अध्ययन का मुख्य जोर डक्टाइल सेगमेंट के भीतर कॉर्ड्स की उपज, डक्टाइल सेगमेंट के बाहर के तत्वों का व्यवहार, कॉलम का व्यवहार, प्लास्टिक के टिका के स्थान पर फ्लैंग्स में बकलिंग और डक्टाइल का व्यवहार था। खंड। परीक्षण फ्रेम ने प्रयोग के दौरान स्थिर हिस्टैरिसिस प्रतिक्रिया प्रदर्शित की यानी 6% स्टोरी ड्रिफ्ट। विशेष खंड के अंत में विवरण ने वांछित स्थानों पर प्लास्टिक का काज सुनिश्चित किया। दूसरे प्रयोग में, स्लैब वाले फ्रेम को भी 6% बहाव तक चक्रीय रूप से लोड किया गया था। स्लैब के साथ फ्रेम पर अध्ययन का मुख्य जोर डक्टाइल सेगमेंट के भीतर कॉर्ड्स की यील्डिंग, डक्टाइल सेगमेंट के बाहर के तत्वों का व्यवहार, कॉलम का व्यवहार, प्लास्टिक के टिका के स्थान पर फ्लैंग्स में बकलिंग, डक्टाइल का व्यवहार था। स्लैब का खंड और दरार प्रसार। स्लैब के साथ परीक्षण फ्रेम ने चक्रीय भार के तहत 6% स्टोरी ड्रिफ्ट तक स्थिर हिस्टैरिसिस प्रतिक्रिया भी दिखाई। कॉलम के पैनेल ज़ोन में डिटेल्डिंग में सुधार किया गया था जिसमें स्टीफ़नर डिटेल्डिंग ने शीयर यील्ड को प्रभावी ढंग से विलंबित किया। स्लैब की उपस्थिति के कारण विशेष खंड के पार्श्व बकलिंग में भी देरी हुई। इस थीसिस में संख्यात्मक और प्रयोगात्मक जांच के निष्कर्षों से निकाले गए निष्कर्ष बताए गए हैं।

TABLE OF CONTENTS

<i>Certificate</i>	<i>i</i>
<i>Acknowledgements</i>	<i>iii</i>
<i>Abstract</i>	<i>v</i>
<i>संक्षेप</i>	<i>vii</i>
<i>Table of Contents</i>	<i>ix</i>
<i>List of Figures</i>	<i>xv</i>
<i>List of Tables</i>	<i>xxv</i>
<i>List of Symbols</i>	<i>xxvii</i>
<i>List of Acronyms</i>	<i>xxxi</i>
CHAPTER 1: INTRODUCTION	1
1.1 General.....	1
1.2 Behavior of Special Truss Moment Frame	7
1.3 Motivation of The Study	8
1.4 Research Objectives and Scope of the Study.....	11
1.5 Organization of Thesis	13
CHAPTER 2: REVIEW OF LITERATURE	15
2.1 General.....	15
2.2 Early Developments of Truss Moment Frames	16
2.3 Recent Developments of STMFs	25
2.3.1 <i>Experimental studies</i>	25
2.3.2 <i>Analytical studies</i>	34
2.3.3 <i>Energy dissipating devices in STMFs</i>	37
2.4 Developments of Code Provisions.....	40
2.5 Design Philosophy for STMF as per Current US Codes	43
2.5.1 <i>General</i>	43
2.5.2 <i>Calculation of Lateral forces in accordance with ASCE 7-16</i>	43
2.5.3 <i>Design Criteria for STMFs in accordance with AISC 341-16</i>	47

2.6	Summary.....	51
CHAPTER 3: DEVELOPMENT AND VALIDATION OF NUMERICAL MODELLING OF STMFs		
53		
3.1	General.....	53
3.2	Background.....	54
3.3	Numerical Modelling of STMFs in PERFORM-3D	54
3.4	Validation of Modelling Technique	59
3.5	Summary.....	65
CHAPTER 4: QUANTIFICATION OF SEISMIC PERFORMANCE FACTORS FOR STMFs.....		
67		
4.1	Introduction	67
4.2	Aim and Objectives	69
4.3	Review of FEMA P695 Methodology.....	70
4.4	Development of System Archetypes	71
4.4.1	<i>Design of archetypes</i>	76
4.4.2	<i>Nonlinear modelling of archetypes</i>	79
4.5	Analysis Results	81
4.5.1	<i>Nonlinear static analysis</i>	81
4.5.2	<i>Nonlinear dynamic analysis</i>	85
4.5.3	<i>Collapse performance assessment</i>	87
4.5.4	<i>Collapse fragility curves</i>	91
4.6	Evaluation of Seismic Performance Factors.....	93
4.6.1	<i>Response modification factor</i>	93
4.6.2	<i>Over-strength factor</i>	95
4.6.3	<i>Deflection amplification factor</i>	95
4.7	Summary.....	96
CHAPTER 5: EFFECT OF SPECIAL SEGMENT ASPECT RATIOS ON SEISMIC COLLAPSE PERFORMANCE OF STMFs.....		
99		
5.1	General.....	99
5.2	Design Philosophy and Performance Evaluation	100
5.2.1	<i>Overview of design guidelines</i>	100
5.2.2	<i>Collapse evaluation methodology</i>	101

5.3	Configuration and Design of STMF Archetypes	102
5.4	Analysis and Results	105
5.4.1	<i>Nonlinear static analysis</i>	106
5.4.2	<i>Nonlinear dynamic analysis</i>	108
5.5	Summary	112
CHAPTER 6: SEISMIC FRAGILITY ASSESSEMENT OF STMFs WITH MULTIPLE VIERENDEEL PANELS.....		113
6.1	Introduction.....	113
6.2	Research Significance	114
6.3	Details of Study Buildings	115
6.3.1	<i>Structural layouts</i>	116
6.3.2	<i>Design of study frames</i>	118
6.3.3	<i>Nonlinear modeling of study frames</i>	122
6.4	Nonlinear Analyses Procedures	126
6.5	Results and Discussion	129
6.5.1	<i>Pushover curves</i>	130
6.5.2	<i>Yielding mechanisms</i>	131
6.5.3	<i>Drift response</i>	131
6.5.4	<i>Spectral acceleration vs. IDR response</i>	133
6.6	Development of Seismic Fragility Curves.....	135
6.7	Summary	139
CHAPTER 7: SEISMIC PERFORMANCE OF HIGH-RISE STMFs WITH MULTIPLE DUCTILE SEGMENTS OF HIGH ASPECT RATIOS.....		143
7.1	Introduction.....	143
7.2	Design and Modelling of Study Frames	144
7.2.1	<i>Structural layout of STMFs</i>	145
7.2.2	<i>Overview of design philosophy</i>	147
7.2.3	<i>Design of study frames</i>	148
7.2.4	<i>Numerical modeling</i>	151
7.3	Nonlinear Static Analyses.....	154
7.3.1	<i>Yield mechanism</i>	155
7.3.2	<i>Base shear vs. roof drift response</i>	155
7.3.3	<i>Yield drifts and maximum plastic rotation</i>	157

7.4	Nonlinear Time-history Analyses.....	160
7.4.1	<i>Performance of STMFs in DBE hazard level.....</i>	163
7.4.2	<i>Performance of STMFs in MCE hazard level.....</i>	167
7.5	Summary.....	170
 CHAPTER 8: QUASI-STATIC TESTING OF SINGLE-STORY STMF WITHOUT FLOOR SLAB		173
8.1	General.....	173
8.1	Experimental Program.....	174
8.1.1	<i>Description of test specimen</i>	174
8.1.2	<i>Material properties</i>	181
8.1.3	<i>Test set-up</i>	182
8.2	Imposed Displacement History	186
8.3	Test Results and Discussion	187
8.3.1	<i>Hysteresis response of the frame.....</i>	188
8.3.2	<i>Behavior of the ductile segment (Special segment).....</i>	189
8.3.3	<i>Behavior of unyielding members of truss girder.....</i>	201
8.3.4	<i>Behavior of connections and columns.....</i>	203
8.3.5	<i>State of strain</i>	210
8.4	Summary.....	218
 CHAPTER 9: QUASI-STATIC TESTING OF SINGLE-STORY STMF WITH FLOOR SLAB		221
9.1	General.....	221
9.2	Experimental Program.....	222
9.2.1	<i>Description of test specimen</i>	222
9.2.2	<i>Material properties</i>	235
9.2.3	<i>Test set-up for STMF with slab</i>	237
9.3	Imposed Displacement History	242
9.4	Test Results and Discussion	242
9.4.1	<i>Hysteresis response.....</i>	243
9.4.2	<i>Behavior of special segment.....</i>	245
9.4.3	<i>Behavior of the unyielding members of the truss girder</i>	254
9.4.4	<i>Behavior of columns and connections.....</i>	255
9.4.5	<i>Behavior of floor slab.....</i>	263

9.4.6	<i>State of strain in the ductile segment</i>	269
9.5	Effectiveness of presence of slab over truss girder.....	277
9.6	Summary	278
 CHAPTER 10: SUMMARY, CONCLUSIONS AND FUTURE RECOMMENDATIONS		281
10.1	Summary	281
10.1.1	<i>Quantification of seismic performance factors for DVSTMF</i>	281
10.1.2	<i>Effect of special segment aspect ratio on collapse performance of STMF</i>	282
10.1.3	<i>Seismic fragility of STMF with multiple ductile Vierendeel panels</i>	282
10.1.4	<i>Seismic performance of high-rise STMF with multiple Vierendeel ductile segment and high panel aspect ratio</i>	283
10.1.5	<i>Slow cyclic testing of single story STMF frame only</i>	283
10.1.6	<i>Slow cyclic testing of single story STMF frame with composite slab</i>	284
10.2	Conclusions.....	284
10.2.1	<i>Quantification of seismic performance factors for DVSTMF</i>	284
10.2.2	<i>Effect of Special segment aspect ratio on collapse performance of STMF</i>	285
10.2.3	<i>Seismic fragility of STMF with multiple ductile Vierendeel panels</i>	286
10.2.4	<i>Seismic performance of high-rise STMF with multiple Vierendeel ductile segment and high panel aspect ratio</i>	287
10.2.5	<i>Slow cyclic testing of single story STMF frame only</i>	288
10.2.6	<i>Slow cyclic testing of single story STMF frame with composite slab</i>	289
10.3	Scope for Future Study	291
 APPENDIX-I		293
 REFERENCES		305
 ANNEXURE		315

LIST OF FIGURES

Figure 1.1: A view of Tru-Frame of Raley Field	5
Figure 1.2: A typical True-Frame (STMF with X-diagonal)	5
Figure 1.3: A typical STMF with 2-panel Vierendeel special segments under construction (Chao and Goel 2006).....	6
Figure 1.4: Ductwork through a Vierendeel special segment opening of an STMF (Chao and Goel 2006)	6
Figure 1.5: Typical configuration and yield mechanism of STMF with (a) X-diagonal and (b) Vierendeel panel (Basha and Goel 1994).....	7
Figure 1.6: Typical configuration and yield mechanism of Vierendeel STMF with (a) single IVM and (b) two IVMs.....	8
Figure 2.1: Typical Detail of test set-up for a TMF with single diagonals (Itani and Goel 1991)	17
Figure 2.2: Typical hysteretic loops for a TMF with single diagonals (Itani and Goel 1991)	17
Figure 2.3: Full span truss with X-diagonal in special segment (Itani and Goel 1994b) ...	20
Figure 2.4: Hysteretic response of a STMF with X-diagonals (Itani and Goel 1994b)	20
Figure 2.5: Test Setup of STMF of Vierendeel special segment (Basha and Goel 1994)..	22
Figure 2.6: Hysteretic loop of STMF with Vierendeel segment (Basha and Goel 1994) ..	22
Figure 2.7 Test setup of STMF (X-diagonals) with slab (Aslani and Goel 1998)	23
Figure 2.8 Details of the test specimen for combined loading (Aslani and Goel 1998)	24
Figure 2.9: Built-up section using double angles as chord members	26
Figure 2.10: Test Setup for cyclic testing on double channel built-up chord members (Parra- Montesinos et al. 2006a).....	27
Figure 2.11: Improved Double channel connection for LTB prevention (Jiansinlapadamrong et al. 2018)	28
Figure 2.12: Test Specimen STMF with single Vierendeel panel SS (Chao et al. 2020) ..	29
Figure 2.13: Test Set-up for STMF with Multiple Vierendeel panel special segment and detail of connection of Intermediate vertical members (Chao et al. 2020)...	30
Figure 2.14: Plastic hinges in the special segment during testing of single Vierendeel panel and multiple Vierendeel panel special segments (Chao et al. 2020)	31
Figure 2.15: Hysteretic response of STMF with (a) single Vierendeel panel SS and (b) multiple Vierendeel panel special segments (Chao et al. 2020)	31
Figure 2.16: General moment-rotation model of double-channel built-up member and general plastic hinge model in commercial software (Chao et al. 2020).....	32

Figure 2.17: STMF sub-assembly overall dimension and test setup (Simasathien et al. 2017).....	33
Figure 2.18: Hysteresis response of sub-assembly (Simasathien et al. 2017).....	34
Figure 2.19: STMF subassembly with two-panel Vierendeel SS (Jordan et al. 2007)	35
Figure 2.20: FE model and boundary condition in ABAQUS (Jiansinlapadamrong et al. 2019).....	37
Figure 2.21: Deformed shape at member rotation demand of 0.02 rad (a) without axial load and (b) with axial load ($P/P_{cr} = 0.3$) (Jiansinlapadamrong et al. 2019).....	37
Figure 2.22: A typical STMF resistance force diagram under lateral forces	41
Figure 2.23: Typical forces acting on elastic segment, (a) Exterior column (lateral forces acting on the right side), (b) Interior column and (c) Exterior column (lateral forces acting towards left)	50
Figure 3.1: Element model in Perform-3D for (a) Floor columns except 1st floor; (b) 1st floor columns; (c) Chord members; (d) Diagonals and (e) Vertical members	56
Figure 3.2: Generalized force-deformation relationship (ASCE/SEI 41-13).....	56
Figure 3.3: Component model: (a) moment-plastic rotation relationship and (b) axial force–bending moment interaction of members within special segment	58
Figure 3.4: Typical 6-story STMFs model in Perform-3D with gravity columns	59
Figure 3.5: Built-up section using double angles and flat bars (Goel et al. 1998).....	60
Figure 3.6: Moment-rotation relationship for chord members of special segment.....	60
Figure 3.7: Typical backbone curve of double-channel element elements for C10X25 (Chao and Goel 2006, 2008)	61
Figure 3.8: Numerical model of STMF with Vierendeel special segment.....	62
Figure 3.9: Deformed shape and yielding of special segment elements of STMF at 5% drift level	62
Figure 3.10: (a) Comparison of pushover curve with test results, (b) Predicted force-deformation curve of STMF without IVMs	63
Figure 3.11: Numerical model of STMF with multiple Vierendeel panels	64
Figure 3.12: Deformed configuration and yielding mechanism of STMF with IVMs	64
Figure 3.13: (a) Comparison of pushover curve with test results, (b) Predicted force-deformation curve of STMF with IVMs	65
Figure 4.1: Schematic representation of a steel truss-moment frame, (b) Desired hinge mechanism of STMFs under lateral loading condition	68
Figure 4.2: Illustration of seismic performance factors: (a) Design-basis earthquake level (FEMA 450, 2003), (b) Collapse-level earthquake level (FEMA P695, 2009).....	69
Figure 4.3: Plan dimensions of the buildings having bay width of (a) 9.16 m, (b) 13.74 m and (c) 18.32 m considered in Set-I archetypes	73

Figure 4.4: Configuration of STMFs in Set-I archetypes buildings having bay width of (a) 9.16 m, (b) 13.74 m, and (c)18.3 m (Aspect ratio of special segment = 2) ... 74

Figure 4.5: Details of Set-II archetypes: (a) Building plan, and (b) configuration of special segments of STMFs 75

Figure 4.6: Three configurations of special segments considered in Set-II archetypes 76

Figure 4.7: Built-up channel section for (a) members within the special segment (b) chord members outside SS with extra web plate 78

Figure 4.8: Forces acting on columns and associated truss girders (a) Exterior column (lateral forces acting on the right side), (b) Interior column and (c) Exterior column (lateral forces acting towards the left side)..... 79

Figure 4.9: (a) Axial force (P)-bending moment (M) interaction of members and (b) Moment- plastic rotation characteristics of members within special segments..... 80

Figure 4.10: Numerical modelling of STMFs along with gravity columns: (a) 3_M0, (b) 3_M1 and (c) 3_M2 81

Figure 4.11: Lateral strength vs. roof drift response of set-I archetypes: (a) 1-story, (b) 3-story and (c) 6-story 83

Figure 4.12: Lateral strength-roof drift response of set-II archetypes: (a) 3-story; (b) 6-story; (c) 9-story and (d) 15-story 84

Figure 4.13: (a) Response spectra of ground motions and (b) IDA response of 6_M0_30_6..... 86

Figure 4.14: IDA response plot of spectral acceleration vs. peak IDR 87

Figure 4.15: Collapse fragility curve for RTR and total uncertainty of Set-I archetypes .. 92

Figure 4.16: Collapse fragility curve for RTR and total uncertainty of Set-II archetypes . 93

Figure 5.1: Plan of STMF archetype with of special segment aspect ratio of 2.5..... 103

Figure 5.2: Elevation of STMF archetype with of special segment aspect ratio of 2.5 ... 103

Figure 5.3: Configuration of truss girder with different aspect ratio of special segment. 104

Figure 5.4: Base shear vs roof drift of archetypes 107

Figure 5.5: response spectra of far-field record set 108

Figure 5.6: IDA response plot of B5_AR_3.0..... 110

Figure 5.7: Collapse fragility curves of the archetypes 111

Figure 6.1: Typical layout and yield mechanism of STMFs with (a) single and (b) multiple Vierendeel panels in the special segments..... 114

Figure 6.2: Floor plan of the study buildings 116

Figure 6.3: Three different configurations of truss girders with (a) No IVM, (b) Single IVM, and (c) Two IVMs in the special segments..... 117

Figure 6.4: Elevation of the 6-story building frames consisting of (a) single (b) double and (c) triple ductile Vierendeel panels in the special segments 118

Figure 6.5: Cross-section details of chord elements of truss girders: (a) within the special segment, (b) outside the special segment..... 120

Figure 6.6: Elements modeling in PERFORM-3D	122
Figure 6.7: (a) Generalized force-deformation relationship (ASCE/SEI 41-13) and (b) Hysteretic response with backbone curve from test results of double-channel section (Chao et. al, 2020).....	125
Figure 6.8: Modelling curves for the elements for (a) Axial – moment interaction and (b) Moment-plastic rotation of the elements within special segments.....	125
Figure 6.9: Numerical models of 6-story study frames with gravity columns: (a) 6_M0; (b) 6_M1 and (c) 6_M2.....	126
Figure 6.10: (a) Comparison of median response spectra with the code specified design spectrums of DBE and MCE levels, (b) Median MCE response spectra for site class D and scaled intensity of median spectra at the fundamental period of 9_M0 study frame.....	129
Figure 6.11: Comparison of pushover curves of the study frames.....	130
Figure 6.12: Formation of plastic hinges in yielding elements for (a) 3_M0 at 1.51%; (b) 3_M0 at 2.61%; (c) 3_M2 at 1.26% and (d) 3_M2 at 1.94% roof drift	132
Figure 6.13: IDA results of study frames: Spectral acceleration vs. peak IDR response .	134
Figure 6.14: Fragility curves of STMFs at three performance levels along with the corresponding median period-based spectral accelerations	137
Figure 7.1: Structural plan of the building considered in this study	144
Figure 7.2: Structural layout of the truss girders in STMFs: (a) Special segment with single Vierendeel panel (Type- A), (b) Special segment with one intermediate vertical member (Type-B), and (c) Special segment with two intermediate vertical members (Type-C).....	146
Figure 7.3: Elevation views of 9-story STMF archetypes: (a) A-9 (Vierendeel panel as the special segment), (b) C-9 (special segments with two intermediate vertical members)	147
Figure 7.4: Numerical models of 9-story STMFs developed in PERFORM-3D: (a) A-9, (b) B-9, and (c) C-9.....	152
Figure 7.5: Yielding of members within SS of study frames: (a) Frame A-9 at 0.58% drift level, (b) Frame A-9 at 3.06% drift level, (c) Frame C-9 at 0.48% drift level; and (d) Frame C-9 at 2.64% drift level.....	156
Figure 7.6: Comparison of pushover curves of (a) 3-story, (b) 6-story, (c) 9-story, (d) 15-story STMFs	157
Figure 7.7: Comparison of mean response spectra of unscaled and scaled ground motions with the code-based spectrums: (a) DBE hazard level, (b) MCE hazard level	160
Figure 7.8: Moment vs. hinge rotation of (a) 3rd story Top chord and (b) 6th story top chord for A-9 study frames under LA09 (DBE Level) and LA21(MCE level) ground motion.....	161
Figure 7.9: Variation of mean interstory drift ratio over the heights of STMFs under DBE level ground motions: (a) 3-story, (b) 6-story, (c) 9-story, (d) 15-story	163

Figure 7.10: Maximum plastic rotation of (a) SS-chords and (b) IVMs of study frames under DBE level ground motions 165

Figure 7.11: Variation of mean interstory drift ratio over the height of STMFs under MCE level ground motions: (a) 3-story, (b) 6-story, (c) 9-story, (d) 15-story 168

Figure 7.12: Maximum plastic rotation of (a) SS-chords and (b) IVMs of study frames under MCE level ground motions 171

Figure 8.1: Test frame with detailed dimensions 177

Figure 8.2: Detailed dimensions of half of truss-girder (All dimensions are in mm) 177

Figure 8.3: Dimensions of plates used in fabrication (All dimensions are in mm) 178

Figure 8.4: Detailed dimensions of web plates added to column and the connection elements of column and load transfer beam (all dimensions are in mm) 178

Figure 8.5: Test frame fabricated with North-facing channels only 180

Figure 8.6: Fabrication of test frame (lying on the ground) with South-facing channels 180

Figure 8.7: Pinned supports at the base of columns 181

Figure 8.8: (a) Tension testing of steel coupon using Universal Testing Machine (UTM) and (b) Tensile stress-strain response of coupons of ISMC 125 182

Figure 8.9: Schematic front view of test set-up 183

Figure 8.10: Schematic top view of test set-up 183

Figure 8.11: Schematic view of test set-up 184

Figure 8.12: Details of specimen and test set-up 185

Figure 8.13: Actuator (attached to one leg of U-Frame) connection to load-transfer beam (Picture taken from back side) 185

Figure 8.14: Actuator connection and roller support for load transfer beam 186

Figure 8.15: Imposed displacement history 187

Figure 8.16: Hysteresis response of test frame under cyclic loads 189

Figure 8.17: Yielding of chords within special segment at 1% drift level 190

Figure 8.18: Yielding of chord within special segment at 1.5% drift level (1st positive peak) 192

Figure 8.19: Yielding of chord within special segment at 1.5% drift level (3rd positive peak) 192

Figure 8.20: State of truss girder at 1.5% drift level 193

Figure 8.21: State of yielding within special segment at 2% drift level 193

Figure 8.22: State of yielding of bottom chord within special segment at 2% drift level (image taken from bottom) 194

Figure 8.23: Buckling of flanges at the end of chord of special segment at 3% drift level 194

Figure 8.24: State of yielding within SS chord within SS at 3% drift level 195

Figure 8.25: Buckling of flanges at the end of SS-Chord at 4% drift level 196

Figure 8.26: Lateral buckling of truss girder within special segment at 4% drift level 196

Figure 8.27: State of yielding of bottom chord within SS at 4% drift level..... 198

Figure 8.28: Buckling of flanges at the end of SS-Chord at 5% drift level 198

Figure 8.29: State of yielding of bottom chord within SS at 6% drift level..... 199

Figure 8.30: Buckling of flanges at the end of SS-Chord at 6% drift level 199

Figure 8.31: Lateral torsional buckling of truss girder within SS at 6% drift level 200

Figure 8.32: State of yielding of chords within SS at various drift level 201

Figure 8.33: State of members outside of the special segment at 6% drift level 202

Figure 8.34: state of side support plates during experiment 204

Figure 8.35: state of chord column connecting gusset plates during experiment 205

Figure 8.36: state of weld of gusset plate and stitch after 6% drift level 205

Figure 8.37: State of flange of column at 0.75% drift level..... 206

Figure 8.38: State of column web and flange at 0.75% drift level..... 207

Figure 8.39: State of column web and flange at 1% and 1.5% drift level..... 208

Figure 8.40: State of web and flange of East column at 6% drift level 209

Figure 8.41: State of web and flange of West column at 6% drift level 209

Figure 8.42: Locations of installed strain gauges and string pot..... 211

Figure 8.43: Locations of installed strain gauges within SS 211

Figure 8.44: Strain gauge data for the SS-top chord (east end) North Facing Channel (left) and South Facing Channel..... 213

Figure 8.45: Strain gauge data for the SS-top chord (west end) North Facing Channel (left) and South Facing Channel (right)..... 213

Figure 8.46: Strain gauge data for the SS-bottom chord (east end) North Facing Channel (left) and Channel-South Facing (right) 214

Figure 8.47: Strain gauge data for the SS-bottom chord (west end) North Facing Channel (left) and South Facing Channel (right)..... 214

Figure 8.48: Strain gauge data for SS-Top Chord (left) and SS-Bottom chord (right), placed in the middle of the web of ductile segment..... 215

Figure 8.49: State of strain in the vertical member just outside the ductile panel 215

Figure 8.50: State of strain in the diagonal member near (a) column (b) ductile segment..... 216

Figure 8.51: State of strain in non-yielding top chord members near (a) column (b) ductile segment..... 216

Figure 8.52: State of strain in the non-yielding bottom chord near (a) column (b) ductile segment..... 217

Figure 8.53: Displacements at the end of special segment during experiment 218

Figure 9.1: Front view showing Vierendeel panel of Test frame with slab without lateral support 224

Figure 9.2: Isometric view of Test frame with slab only without lateral support 224

Figure 9.3: Test specimen with dimensions of STMF with slab 225

Figure 9.4: Detailed dimensions of half of truss-girder of test specimen (All dimensions are in mm)..... 225

Figure 9.5: Detailed dimensions of Plates used in fabrication of test specimen (All dimensions are in mm)..... 226

Figure 9.6: Detailed dimension of web plates added to column and the connection elements of column and load transfer beam (all dimensions are in mm) 226

Figure 9.7: Test frame fabricated with North Facing channels only 227

Figure 9.8: Fabrication of Test frame (lying on the ground) with south facing channels 228

Figure 9.9: Arrangements of shear connector and reinforcements in slab 230

Figure 9.10: Images during casting of slab on test frame..... 231

Figure 9.11: Images taken from (a) East end and (b) West end of slab on test frame 232

Figure 9.12: Images taken from (a) West end (upper) and (b) East end (Lower) of test specimen 233

Figure 9.13: Pinned supports at the base of the columns for test specimen 234

Figure 9.14: (a) Steel coupon testing using UTM and (b) Tensile Stress-Strain Curve of Coupons 235

Figure 9.15: Testing of cylindrical concrete specimen..... 236

Figure 9.16: Schematic front view of test set-up..... 237

Figure 9.17: Schematic top view of test set-up 238

Figure 9.18: Schematic isometric view of test set-up..... 239

Figure 9.19: Details of test specimens and set-up 240

Figure 9.20: Actuator (attached to one leg of U-Frame) connection to load-transfer beam (Picture taken from back side)..... 241

Figure 9.21: Actuator connection and roller support for load transfer beam 241

Figure 9.22: Hysteresis response of test frame under cyclic loads and Capacity curve... 244

Figure 9.23: State of ductile Vierendeel panel of special segment at 1% drift level..... 246

Figure 9.24: State of yielding within special segment at 1.5% drift level..... 246

Figure 9.25: State of yielding within special segment at 1.5% drift level in the channel at bottom chord 247

Figure 9.26: State of yielding within special segment at 2% drift level (Front view)..... 248

Figure 9.27: State of yielding within special segment at 2% drift level (View from bottom side)..... 248

Figure 9.28: State of yielding within special segment at 3% drift level..... 249

Figure 9.29: State of buckling of flanges within special segment at 3% drift level..... 250

Figure 9.30: Yielding and buckling of flanges within special segment at 4% drift level 251

Figure 9.31: Yielding within special segment at 4% drift level (View from bottom side)	252
Figure 9.32: Yielding and buckling of flanges within special segment at 5% drift level	252
Figure 9.33: Lateral buckling of truss girder at 5% drift level.....	253
Figure 9.34: State of yielding and buckling of flanges within SS at 6% drift level.....	253
Figure 9.35: Lateral buckling of truss girder within SS at 6% drift level	254
Figure 9.36: State of ductile segment at various drift levels of STMF with slab.....	254
Figure 9.37: State of unyielding members at 6% drift level of STMF with slab	255
Figure 9.38: State of Column at 0.75% drift level in the panel zone	256
Figure 9.39: State of flange of the column at 0.75% drift level at the level of slab.....	257
Figure 9.40: State of flange of the column at 1% drift level below the bottom chord.....	257
Figure 9.41: State of inner flange of the column at 1.5% drift level.....	257
Figure 9.42: State of web of the column at 1.5% drift level	258
Figure 9.43: Shear marks on the inner flange of the column at 5% drift level	259
Figure 9.44: State of flange of the column at 5% drift level	259
Figure 9.45: Whitewash flaking marks on the column at 6% drift level	260
Figure 9.46: Column base at 6% drift level	261
Figure 9.47: Whitewash flaking marks in the panel zone at various drift level.....	262
Figure 9.48: Positions of video camera installed for observation of surface of slab	264
Figure 9.49: Top surface of the slab viewed from the video cameras	264
Figure 9.50: Cracks in the slab at 0.75% drift.....	265
Figure 9.51: Crack in slab and state of corrugated sheet at 1.5% drift	265
Figure 9.52: State of corrugated sheet at 3% and 4% drift	266
Figure 9.53: Crack in slab at 5% drift	266
Figure 9.54: State of slab with corrugated sheet at 5% drift.....	266
Figure 9.55: Crack in the slab at 6% drift	267
Figure 9.56: State of shear connector within SS at 6% drift	268
Figure 9.57: State of slab at 6% drift	268
Figure 9.58: Locations of strain gauges installed within ductile segment	270
Figure 9.59: Locations of strain gauges installed outside ductile segment.....	270
Figure 9.60: Strain gauge data for SS top chord at east end for (a) North facing channel and (b) South facing channel.....	271
Figure 9.61: Strain gauge data for SS top chord at west end for (a) North facing channel and (b) South facing channel.....	271
Figure 9.62: Strain gauge data for SS bottom chord at east end for (a) North facing channel and (b) South facing channel.....	272

Figure 9.63: Strain gauge data for SS bottom chord at west end for (a) North facing channel and (b) South facing channel 272

Figure 9.64: Strain gauge data for (a) SS top chord and (b) bottom chord placed in the middle of the web of ductile segment 273

Figure 9.65: Strain gauge plot for the vertical member just outside the ductile segment 274

Figure 9.66: plot of strain gauge data for the diagonal members placed near (a) Column and (b) ductile segment..... 274

Figure 9.67: Plot of strain gauge data for un-yielding top chord near (a) Column and (b) ductile segment 275

Figure 9.68: Plot of strain gauge data for un-yielding bottom chord near (a) Column and (b) ductile segment 276

Figure 9.69: Displacements at the ends of the ductile segment during experiment 277

Figure 9.70: Envelopes of Capacity curve of the test specimens 278

LIST OF TABLES

Table 1.1: Details of building using STMF with X-diagonal (Tru-Frame) (Source: http://www.thespectrusgroup.com/projects/index.html)	4
Table 1.2: Comparison of time and cost of moment frame, braced frame, and Tru-frame (Source: http://www.thespectrusgroup.com)	5
Table 4.1: Summary of the characteristics of archetypes	75
Table 4.2: Summary of seismic design parameters selected for the design of archetypes	77
Table 4.3: Summary of design parameters of archetypes derived from pushover curves	85
Table 4.4: Computation of collapse margin ratios of archetypes	88
Table 4.5: Performance check for a group of archetypes	96
Table 5.1: Seismic Design parameters for 9-story STMF	105
Table 5.2: Summary of member size for archetype B5_AR_3.0	105
Table 5.3: Summary of nonlinear static analysis results	108
Table 5.4: Summary of nonlinear Dynamic analysis and performance check	111
Table 6.1: Summary of geometric characteristics of the study frames	118
Table 6.2: Design base shear and time periods of study frames	119
Table 6.3: Member sizes of elements in the special segments of all study frames	123
Table 6.4: Ground motion characteristics of earthquake records (FEMA P695 2009)	128
Table 6.5: Scale factor for the Ground motion anchored at MCE level	129
Table 6.6: Roof drift levels corresponding to various limit states of the study frames	133
Table 6.7: Median spectral acceleration and standard deviation of study frames	138
Table 6.8: Probability of exceeding the performance levels of study frames under DBE and MCE hazard levels	139
Table 7.1: Seismic design parameters considered in the design of study buildings	149
Table 7.2: Fundamental time period and design base shear of study frame	149
Table 7.3: Summary of member sizes of 3-story study frames	150
Table 7.4: Summary of member sizes of 9-story study frames	150
Table 7.5: Computed time period and base shear vs fundamental time period from modal analysis and maximum base shear from Pushover curve for the study STMFs	151
Table 7.6: Comparison of Expected vertical shear in SS calculated and developed for 9-story STMFs	154
Table 7.7: Summary of yielding roof drifts and maximum plastic rotation of members in special segments of 3-, 6- and 9-story STMFs	158
Table 7.8: Characteristics of SAC DBE Level ground motions (LA01 to LA20)	162

Table 7.9: Characteristics of SAC MCE level ground motions (LA21 to LA40).....	162
Table 7.10: Mean peak plastic rotation demand on members of special members of 3-story study STMFs under DBE and MCE level ground motions.....	164
Table 7.11: Mean peak plastic rotation demand on yielding members of 6-, 9- and 15-story STMFs under DBE and MCE level ground motions	166
Table 8.1: Scaling factors using test specimen dimension and section properties.....	175
Table 8.2: Dimension of cross-section of columns and truss girder	176
Table 9.1: Material Properties of Coupons of ISMC 125	236

LIST OF SYMBOLS

$ACMR_{10\%}$	Acceptable value of the adjusted collapse margin ratio (ACMR), on average, for the performance group of interest
$ACMR_{20\%}$	Acceptable value of the adjusted collapse margin ratio (ACMR) for an individual archetype of the performance group of interest
A_g	Gross cross-sectional area
B_l	Numerical coefficient for effective damping and the fundamental time period of the structure
C_d	Deflection amplification factor
C_s	Seismic response coefficient
C_u	Coefficient for the upper limit on the calculated time period
C_{vx}	Vertical distribution factor
D_l	Plastic rotation at ultimate strength
D_r	Plastic rotation at strength loss
D_u	Plastic rotation at strain hardening
E	Modulus of elasticity of structural steel
F_a	Short-period site coefficient
$F_d(S_{aT})$	Fragility function for damage state, d evaluated at spectral acceleration, S_{aT}
F_i	Lateral force at i^{th} floor
F_v	Long-period site coefficient
F_{ye}	Expected yield strength of material
F_y	Material yield stress of structural steel
I	Importance factor of the structure
I_c	Moment of inertia of chord member of the special segment
I_v	Moment of inertia of intermediate vertical member
L	Length of truss girder
L_{pd}	Maximum allowed unbraced length
L_s	length of the special segment
M	Bending moment
M_n	Nominal flexural capacity
M_{nc}	Nominal flexural strength of a chord member of SS

M_{nv}	Nominal flexural strength of intermediate vertical member
M_p	Plastic moment capacity of chord members of the special segment
M_p^*	Ultimate flexural strength of the composite section under monotonic loading
M_u	Ultimate flexural capacity
P	Axial force
P_{cr}	Strength of X-diagonal in compression buckling
P_n	Nominal axial capacity
P_{nc}	Nominal compressive strength of a diagonal member of SS
P_{nt}	Nominal tensile strength of a diagonal member of SS
P_u	Ultimate axial capacity
P_y	Yield-strengths of X-diagonal in tension
P_{ye}	expected axial yield force
R	Response modification factor
R_y	Ratio of the expected yield stress to the specified minimum yield stress
S_{aT}	Particular value of intensity of response spectra
$S_{aT(50\%)}$	Median of the response spectra for a particular damage state
S_{CT}	Median collapse intensity
S_{DS}	Design spectral response acceleration in the short period range
S_{D1}	Design spectral response acceleration at a period of 1.0 s
S_{MS}	Maximum considered earthquake spectral acceleration at short period
S_{MT}	MCE intensity at the fundamental period
S_{M1}	Maximum considered earthquake spectral acceleration at one second
S_s	Mapped maximum considered earthquake spectral response acceleration at short period
S_T	Period based spectral acceleration
S_1	Mapped maximum considered earthquake spectral response acceleration at one second
T	Calculated time period of structure
T_L	Long-period transition period
T_1	Fundamental time period of structure determined from eigenvalue analysis
V_{db}	Design base shear of the structure
V_E	Elastic base shear
V_{max}	Maximum base shear
V_{ne}	Expected shear strength of special segment

V_p	Ultimate shear capacity of special segment
V_{ult}	Ultimate shear capacity of SS considering composite action
W	Effective seismic weight of the structure
Z_p	Plastic section modulus
b	Width of flange
d	A particular value of d_s
d_s	Damage state at performance levels
h	Depth of web
h_i	Height from the base of structure to i^{th} level
h_x	Height from the base of structure to level x
l	Length of element
l_c	Length of column
m	Number of intermediate vertical member
r_y	Radius of gyration of individual component about the weak (y) axis
t_w	Thickness of web
t_f	Thickness of flange
w_x	Seismic wt of the structure at level x
w_i	Seismic wt. of the structure at i^{th} level
α	Angle made by X-diagonals with the horizontal
β	Ratio of cyclic flexural strength to monotonic flexural strength
β_{DR}	Design related collapse uncertainty
β_{MDL}	Modeling related collapse uncertainty
β_{RTR}	Record-to-record collapse uncertainty
β_{TD}	Test data related collapse uncertainty
β_{TOT}	Total system collapse uncertainty
δ	Design elastic displacement
δ_E	Expected inelastic displacement
δ_u	Roof displacement corresponding to 80% of maximum base shear strength
$\delta_{y,eff}$	Effective yield displacement
λ_{DR}	Random variable representing design requirements-related collapse uncertainty
λ_{MDL}	Random variable representing modeling-related collapse uncertainty
λ_{RTR}	Random variable representing record-to-record collapse uncertainty
λ_{TD}	Random variable representing test data-related collapse uncertainty

ϕ	Ratio of post-buckling to initial buckling strength of X-diagonals
$\phi_{1,r}$	Ordinates of the fundamental mode at roof level
$\phi_{1,x}$	Ordinates of the fundamental mode at floor level x
θ_p	Roof drift ratio
θ_y	Yield rotation
Ω	Overstrength factor

LIST OF ACRONYMS

AR	Aspect Ratio
ACMR	Adjusted collapse margin ratio
BRBs	Buckling restrained braces
BRBTMF	Buckling restrained braced truss moment frame
BRKBTMF	Buckling restrained knee braced truss moment frame
CBFs	Concentrically braced frames
CMR	Collapse margin ratio
CP	Collapse Prevention
CT-CP	Column truss connecting plate
DBE	Design basis Earthquake
DL	Dead Load
DR	Design requirements uncertainty
DTMFs	Dissipative truss moment frames
DVSTMF	Ductile Vierendeel steel special truss moment frame
EBF	Eccentrically braced frame
EDDs	Energy dissipation devices
ED-CGL	Elastic Design-Chao Goel distribution
ED-IT	Elastic design with Inverted Triangular distribution
ELF	Equivalent lateral force
FE	Finite element
FF	Far-Field
FLB	Flange local buckling
FTMF	Fused truss moment frame
GP	Gusset plate
IDA	Incremental dynamic analysis
IDR	Inter-story drift ratio
IO	Immediate Occupancy
ISMB	Indian standard medium weight beam
ISMC	Indian standard medium weight channel
IVMs	Intermediate vertical members

LL	Live load
LS	Life safety
LTB	Lateral torsional buckling
MCE	Maximum Considered Earthquake
MDL	Modelling uncertainty
MRF	Moment-resisting frame
OMRF	Ordinary moment-resisting frame
PBPD	Performance based plastic design
PD	Plastic design
PG	Performance group
RTR	Record-to-record uncertainty
SDC	Seismic Design Category
SMFs	Steel moment frames
SS	Special segment
SSF	Spectral shape factor
STMF	Special Truss Moment frame
TD	Test data uncertainty
TMF	Truss Moment Frame
UTM	Universal testing machine